

# Direct method for reconstructing shape from shading

John Oliensis† and Paul Dupuis‡

Department of Computer Science†  
University of Massachusetts at Amherst  
Amherst, Massachusetts 01003

Box F, Division of Applied Mathematics‡  
Brown University  
Providence, Rhode Island 02912

## Abstract

A new approach to shape from shading is described, based on a connection with a calculus of variations/optimal control problem. The approach leads naturally to an algorithm for shape reconstruction that is simple, fast, provably convergent, and, in many cases, provably convergent to the correct solution. In particular, if the surface is known to be locally concave (or convex) at a singular point in the image, then the algorithm provably reconstructs the correct surface in a region around the singular point. The algorithm is robust against noise and, in contrast with standard variational algorithms, does not require regularization. An explicit representation is given for the surface: its height is expressed as the minimal cost for an optimally controlled trajectory. This representation makes the convergence analysis for the algorithm transparent, and allows it to be easily adapted to different situations in practice. Uniqueness of the reconstruction (under suitable conditions) is an immediate consequence. We focus primarily on the case of illumination from the camera direction. For this case, if the singular points at which the surface is locally concave have been identified, and their heights are known, then the algorithm provably reconstructs the original imaged surface. For general direction of illumination, there is a representation of the surface in terms of a differential game, and a slightly modified surface reconstruction algorithm. Finally, given a continuous image, the algorithm can be proven to converge to the continuous surface solution as the image sampling frequency is taken to infinity.

## 1. Introduction

Shape from shading has traditionally been considered an ill-posed problem, with potentially infinitely many different surfaces corresponding to a shaded image. Therefore, most algorithms for reconstructing shape have incorporated *regularization* techniques to guarantee recovery of a unique, 'physically reasonable' surface solution.

More recently, it was suggested that shape from shading need not be ill-posed when the image contains singular points, i.e., maximally bright image points [1,4,14,15,12,11]. This was shown for the case of illumination from—or symmetric around—the camera direction in [12]. In addition, a general shaded image was shown to *uniquely* determine shape under the assumed lighting conditions [12]. Singular points provided the essential constraints.

Singular points continue to give strong constraints on the surface solutions for illumination from a general direction [11]. Thus, shape from shading should not be assumed ill-posed in general, and regularization should be used with caution. Also, the image of the occluding boundary gives no useful constraint on surface reconstruction [11]. Singular points, therefore, provide the primary constraints.

Nevertheless, shape-from-shading algorithms in the past have not taken full advantage of the strong constraints due to singular points. Algorithms based on the method of characteristic strips [3] have used these constraints explicitly, but in an approximate way. This class of algorithms has usually been applied to rather simple images, and suffers from nonrobustness in the presence of noise.

Most recent algorithms for recovering shape from shading have been based on the variational approach (e.g., [6,5,4]). These algorithms have had significant successes on complex images, but do not explicitly use the singular point constraints. This is seen experimentally in the fact that these algorithms do better on

complicated images with many singular points than on simple images with just one singular point (see below and also [9]); yet for such simple images, the sole singular point is known to directly and uniquely constrain the surface reconstruction [1,15].

In this paper, an algorithm is presented that takes full advantage of the singular point constraints. It is simple, fast, provably convergent, and, in many cases, provably convergent to the correct solution. In particular, if the surface is known to be *unimodal* at a singular point in the image (i.e., locally concave or convex at this point), then the algorithm provably reconstructs the correct surface in a region around the singular point. The algorithm is robust against noise and, unlike previous algorithms, does not employ regularization. There is no problem with false minima, in contrast to the standard variational approach. Finally, this approach is capable of dealing with some orientation discontinuities—images for which the intensity function is only piecewise continuous.

The algorithm is based on establishing the equivalence of shape from shading to a calculus of variations/optimal control problem. This can be done for illumination from the camera direction, or for regions near unimodal singular points. For the general case with illumination from an arbitrary direction, the optimal control problem must be extended to a differential game. This equivalence facilitates the theoretical analysis of shape from shading, and makes the algorithm highly adaptable in practice. It also gives intuition about the convergence performance of the algorithm. Below, we present a simple uniqueness proof for shape from shading which generalizes from the local uniqueness results of Bruss [1] and Saxberg [15]. This is possible because, in the optimal control representation, an expression for the surface corresponding to a shaded image can be exhibited explicitly.

## 2. Shape from Shading as a Problem of Optimal Control: Heuristic Derivation

The imaged surface is assumed to be Lambertian, and viewed from above: the optical axis points in the  $-\hat{z}$  direction. It is represented in the explicit form  $z(x, y)$ , where  $z : \mathbf{R}^2 \rightarrow \mathbf{R}$  is the *height function* to be reconstructed. We consider first the simpler case of illumination along the viewing direction  $-\hat{z}$  (vertical light). The case of illumination from a general direction will be discussed later.

Under these conditions, the image irradiance equation is:

$$I(x, y) = \frac{1}{(1 + |\nabla z(x, y)|^2)^{1/2}}. \quad (2.1)$$

It is convenient to rewrite this in the eikonal form:

$$|\nabla z(x, y)|^2 = \frac{1}{(I(x, y))^2} - 1 \equiv V(x, y), \quad (2.2)$$

where  $I(x, y) \in (0, 1]$ ,  $V(x, y) \in [0, \infty)$ . This type of equation arises frequently in the dynamical programming approach to problems of optimal control. In this section, we give a heuristic and indirect demonstration that it is equivalent to a calculus of variations/optimal control problem. Later, a direct and rigorous derivation will be given. Other possibilities (e.g. inclusion of a terminal cost) are also of interest for shape from shading, and will be discussed below.

We consider the following control problem: a 'particle' initially located at  $(x_0, y_0)$  moves in the image plane in response to control parameters  $u, v$ , according to:

$$\dot{x} = u, \quad \dot{y} = v, \quad x(0) = x_0, \quad y(0) = y_0. \quad (2.3)$$

The control parameters are to be chosen to minimize a cost function for the particle's trajectory  $(x(s), y(s))$ :

$$U(x_0, y_0, T) = \inf \frac{1}{2} \int_0^T ds \left( u(s)^2 + v(s)^2 + V(x(s), y(s)) \right). \quad (2.4)$$

In this equation, the minimal cost has been defined as a function of the trajectory starting point  $(x_0, y_0)$ . The infimization is over all piecewise continuous functions  $u(\cdot), v(\cdot)$  on  $[0, T]$ . Let

$$U(x, y) = \lim_{T \rightarrow \infty} U(x, y, T).$$

$U(\cdot)$  will turn out (in the unimodal case) to be the surface  $z(x, y)$  up to a translation. To show this formally, we assume that  $U(\cdot)$  is a differentiable function of the starting point, and formally demonstrate using dynamical programming that it satisfies eq. 2.2.

Let  $\delta T$  be a small time increment. Then:

$$U(x_0, y_0, T) = \inf_{(u,v)} \left[ U(x(\delta T), y(\delta T), T - \delta T) + \frac{1}{2} \int_0^{\delta T} ds \left( u(s)^2 + v(s)^2 + V(x(s), y(s)) \right) \right]. \quad (2.5)$$

The explicit infimization is now over the portion of the trajectory for which  $T \in [0, \delta T]$ ; the infimization over the rest of the trajectory range has been included in the cost function  $U(\cdot, T - \delta T)$ . Since  $\delta T$  is small,  $U$  can be expanded to first order in this quantity, which gives (for  $\delta T \rightarrow 0$ ):

$$\frac{\partial U}{\partial T}(x, y, T) = \inf_{(u(0), v(0))} \left[ \frac{1}{2} \left( u^2(0) + v^2(0) + V(x, y) \right) + \frac{\partial U}{\partial x}(x, y, T)u(0) + \frac{\partial U}{\partial y}(x, y, T)v(0) \right]. \quad (2.6)$$

Performing the minimization over  $u(0)$  and  $v(0)$  yields:

$$u(0) = -\frac{\partial U}{\partial x}(x, y, T), \quad v(0) = -\frac{\partial U}{\partial y}(x, y, T), \quad (2.7)$$

and

$$\frac{\partial U}{\partial T}(x, y, T) = \frac{1}{2} \left[ V(x, y) - \left( \frac{\partial U}{\partial x}(x, y, T) \right)^2 - \left( \frac{\partial U}{\partial y}(x, y, T) \right)^2 \right]. \quad (2.8)$$

Suppose that the image region under consideration is a small neighborhood of a singular point, at which  $I = 1$  and  $V = 0$ . A minimal cost trajectory clearly moves toward regions of smaller  $V$ , and will converge to the singular point at which the incremental cost is zero. As the trajectory converges to this point, the total cost along the trajectory converges to a *finite* value. Therefore, the integration limit  $T$  in eq. 2.4 can be taken to infinity, and  $U(x, y)$  is well defined. Since the time derivative vanishes,  $U(x, y)$  satisfies:

$$\left( \frac{\partial U(x, y)}{\partial x} \right)^2 + \left( \frac{\partial U(x, y)}{\partial y} \right)^2 = V(x, y). \quad (2.9)$$

Since this is just the image irradiance equation, eq. 2.2,  $U(\cdot)$  can be identified with  $z(x, y)$ . Also,  $u$  and  $v$  can be identified with  $-p$  and  $-q$ , respectively, from eq. 2.7. Thus the minimal cost trajectories are curves of steepest descent, and are just the *characteristic strips* [3,11].

Note also that  $U \geq 0$ , and that  $U = 0$  only at the singular point. Thus, the solution that is locally concave at the singular point has been automatically selected by this formulation; the solution locally convex at the singular point is just its negative. The solution  $U$  is unique, since it is equal to the infimum of the cost, which must be unique. Since an infimum of the cost always exists, the solution  $U$  always exists. It must be continuous, but need not be differentiable.

This formulation also gives a way of computing  $U$ . Clearly,  $U(x, y, 0) = 0$  for all  $(x, y)$ , while  $U(x, y, T)$  is monotonically increasing in time: extending a trajectory cannot result in a reduced cost. Therefore, by solving eq. 2.8 iteratively in time, with initial condition  $U(\cdot, T) = 0$  at  $T = 0$ , a sequence of functions

$U(x, y, T)$  is obtained which at every point converges monotonically upward to  $z(x, y)$  as  $T \rightarrow \infty$ . Because this convergence is pointwise monotonic, it is clearly stable.

For the actual implementation, an iterative procedure is used that is justified by its exact relation to a discretized control problem [7]. The continuous image plane is replaced by an image discretized into pixels, and the trajectory described by eq. 2.3 is approximated by a Markov process. This is described in detail in the next section. It can be shown that this gives a discrete approximation  $U^h$  to  $U$ , which converges to the continuous  $U$  as the spatial grid size  $h$  approaches zero. However, a naive discretization of eq. 2.8 does *not* necessarily give a stably convergent algorithm.

### 3. Algorithm Description

We now give a more detailed description of the algorithm and its derivation. We consider a control problem defined on the discrete grid of pixels and chosen to approximate the continuous calculus of variations problem described above.  $h$  is the pixel spacing. For the discrete case, a 'particle' trajectory is a sequence of discrete jumps between grid sites—a poor approximation to a continuous trajectory. In order to better approximate a continuous trajectory on a discrete grid, an element of randomness is introduced.

The control problem is as follows: a 'particle', with initial image plane location  $\phi_0 \equiv (i_0, j_0)h$ , jumps between neighboring pixel sites in response to control parameters  $\mathbf{C} \equiv (u(k), v(k))$ , where  $k$  indicates the time step. (A 4-neighborhood is assumed.) The jumps are probabilistic, but on average

$$\langle \phi(k+1) - \phi(k) \rangle = \Delta t \mathbf{C}(k), \quad (3.10)$$

in analogy with eq. 2.3. Here  $\Delta t$  is the time increment from time step  $k$  to step  $k+1$ , and  $\langle \rangle$  denotes the noise average. Let  $\eta(k)$  be the random vector representing the jump at time  $k$ :  $\eta \equiv \phi(k+1) - \phi(k)$ . The jump probabilities are chosen to be:

$$\begin{aligned} \mathbf{P}(\eta = (\text{sgn}(\mathbf{C}_1), 0)h) &= \Delta t |\mathbf{C}_1| / h, \\ \mathbf{P}(\eta = (0, \text{sgn}(\mathbf{C}_2))h) &= \Delta t |\mathbf{C}_2| / h, \\ \mathbf{P}(\eta = 0) &= 1 - \Delta t (|\mathbf{C}_1| + |\mathbf{C}_2|) / h, \end{aligned} \quad (3.11)$$

with all other probabilities zero. The subscripts 1,2 denote the vector components. Note that  $\Delta t$  and the control parameters must be chosen small enough so that all probabilities are nonnegative and the total probability is unity; and that the jump probability is nonzero only in the quadrant where  $\mathbf{C}$  lies. It is clear that eq. 3.11 implies eq. 3.10.

The analog to the calculus of variations problem is as follows: choose the control parameters to minimize the *expected* cost for the discrete trajectories:

$$U^h(\phi_0, K) = \inf \left\langle \frac{1}{2} \sum_{k=0}^{K-1} \Delta t (\phi(k)) (u(k)^2 + v(k)^2 + V(\phi(k))) \right\rangle, \quad (3.12)$$

where the infimization is over all nonanticipative control sequences  $\{(u(k), v(k)), k = 0, \dots, K\}$ . We have allowed  $\Delta t$  to depend on position. This will cause the algorithm to converge more quickly, as explained later. It can be shown the value function  $U^h$  for this discrete control problem converges to the continuous value function as the grid spacing is taken to zero.

A dynamical programming equation can be derived for this control problem as in the previous section:

$$U^h(\phi_0, K) = \inf_{(u(0), v(0))} \left\{ \frac{1}{2} \Delta t (\phi_0) (u(0)^2 + v(0)^2 + V(\phi_0)) + \langle U^h(\phi_0 + \eta, K-1) \rangle \right\}. \quad (3.13)$$

Let  $D_{a+}$  and  $D_{a-}$  represent the discrete forward and backward partial derivatives for the  $\hat{a}$  direction:

$$D_{a+}U^h(\phi, K) \equiv (U^h(\phi + h\hat{a}, K) - U^h(\phi, K)) / h, \quad D_{a-}U^h(\phi, K) \equiv (U^h(\phi, K) - U^h(\phi - h\hat{a}, K)) / h. \quad (3.14)$$

Then the expectation in the equation above is easily calculated from the probabilities of eq. 3.11:

$$\begin{aligned} \langle U^h(\phi_0 + \eta, K - 1) \rangle &= U^h(\phi_0, K - 1) + \Delta t(\phi_0) \left( u(0) D_{1\text{sgn}(u(0))} U^h(\phi_0, K - 1) \right. \\ &\quad \left. + v(0) D_{2\text{sgn}(v(0))} U^h(\phi_0, K - 1) \right), \end{aligned} \quad (3.15)$$

giving an equation similar to eq. 2.6. Because of the sign functions, the minimization is slightly complicated: the cases with  $\mathbf{C}$  in different quadrants must be treated separately. Also, the minimization is only over a restricted range of  $\mathbf{C}$ , since negative probabilities must be avoided. The final result is analogous to eq. 2.8:

$$U^h(\phi, K + 1) - U^h(\phi, K) = \frac{\Delta t(\phi)}{2} [V(\phi) - \tilde{D}_1 U^h(\phi, K) - \tilde{D}_2 U^h(\phi, K)]. \quad (3.16)$$

This equation represents the basic version of our algorithm for shape reconstruction. The functions  $\tilde{D}_1$ ,  $\tilde{D}_2$  correspond to somewhat unusual discretizations of the squares of the partial derivatives appearing in eq. 2.8:

$$\tilde{D}_a U^h(\phi, K) \equiv \begin{cases} (D_{a+} U^h)^2 & \text{if } D_{a+} U^h, D_{a-} U^h \leq 0, \\ (D_{a-} U^h)^2 & \text{if } D_{a+} U^h, D_{a-} U^h \geq 0, \\ \sup((D_{a+} U^h)^2, (D_{a-} U^h)^2) & \text{if } D_{a+} U^h \leq 0, D_{a-} U^h \geq 0, \\ 0 & \text{if } D_{a+} U^h \geq 0, D_{a-} U^h \leq 0. \end{cases} \quad (3.17)$$

Here, for simplicity, we have neglected the effect of the finite range for  $\mathbf{C}$ .

As before, the initial value for  $U^h(\phi, \cdot)$  may be taken as 0. The right-hand side of eq. 3.16 must always be positive, since the expected cost for an optimal trajectory cannot decrease with time. (This also gives a bound on the minimizing controls, and therefore permits an estimate of the optimal values for  $\Delta t(\phi)$ .) Therefore, an iterative solution  $U^h(\phi, K)$  to this equation increases monotonically at every point.

To avoid indeterminacy, it is necessary to impose the boundary condition that no trajectory exits the image; the significance of this is discussed below. This is easily done. One method is to modify the probabilities of eq. 3.11 at a boundary point so that there is zero probability for a trajectory to move in the forbidden direction; another is described in the next section. Modifying the probabilities causes a slight change in the definitions of  $\tilde{D}_1$ ,  $\tilde{D}_2$  at the boundary points. Assuming this has been done, and that there are singular points in the image where  $V = 0$ , then as  $k \rightarrow \infty$  all optimal trajectories must converge to the singular points. Thus  $U^h(\phi, K)$  converges monotonically as  $k \rightarrow \infty$  to a solution  $U^h(\phi)$  that must satisfy the discretized shape-from-shading equation

$$\tilde{D}_1 U^h(\phi) + \tilde{D}_2 U^h(\phi) = V(\phi), \quad (3.18)$$

which is the analog of eq. 2.2. Of course, this discretization is unusual (e.g., [4]), but the error introduced is of the same order of magnitude as for other discrete approximations of the continuous problem. Generally, one expects that one-sided (as used here) rather than centered discretizations of the derivatives will lead to stable algorithms.

For the solution found by the algorithm of eq. 3.16, the height  $z$  is always nonnegative, since the summand in eq. 3.12 is. Also,  $z = 0$  at a singular point; a trajectory beginning at a singular point achieves minimal cost by remaining there, since  $V = 0$  at the point. Thus,  $z$  attains a local minimum at a singular point.

Also, as in eq. 2.7, the optimal controls away from singular points are given by:

$$u = -D_{1\pm} U^h,$$

$$v = -D_{2\pm}U^h. \quad (3.19)$$

Therefore, from eq. 3.10, the expected optimal trajectories are approximate curves of steepest descent.

The algorithm described in this section is appropriate for *unimodal* images—images containing just one singular point where the height has either a local minimum or maximum. For these images, the iterative solution of eq. 3.16 will correctly reconstruct the original surface at all points where this surface is theoretically determined [11]—that is, at all points connected by a steepest descent curve on the original surface to the singular point. Such points “learn” their height from the singular point. In contrast, at other image points the surface reconstruction can be ambiguous [11]. These ambiguous points lie on steepest descent curves that exit the image rather than terminating at the singular point. Imposing the boundary condition as above that no trajectory exits the image only affects the surface reconstruction at these ambiguous points. Our algorithm does not necessarily reproduce the original surface at ambiguous points.

A modified algorithm appropriate for the multimodal case (many singular points) is described in the next section.

#### 4. Modifications of the Algorithm

The algorithm of eq. 3.16 is of the Jacobi type, with the surface updated everywhere in parallel at each iterative step. Using standard arguments, we expect that the algorithm will also converge if implemented via Gauss-Seidel, with updated surface estimates used as soon as they become available. This should produce a significant speedup for implementation on a serial machine.

A more important modification introduces a *terminal cost* term into the cost function. The terminal cost gives a method for implementing boundary conditions—for instance the condition that no trajectory exits the image—and an algorithm capable of dealing with multimodal images. It is used also in the theoretical proof of Section 5. Including this term, the minimal cost is (compare eq. 3.12):

$$U^h(\phi_0, K) = \inf_{(u,v)} \left\langle g(\phi(K)) + \frac{1}{2} \sum_{k=0}^K \Delta t(\phi(k)) \left( u(k)^2 + v(k)^2 + V(\phi(k)) \right) \right\rangle. \quad (4.20)$$

The terminal cost,  $g(\phi(K))$ , introduces a penalty term for a trajectory stopping at the position  $\phi(K)$ . It causes an optimal trajectory to not remain in regions of high terminal cost, and converge instead to points of low terminal cost. This can dramatically improve the convergence speed of the algorithm. Also, the terminal cost can be used to distinguish between singular points of different type (concave, convex, saddle). In the eventual surface solution, only a concave-type singular point should be the terminus for an optimal trajectory, since it is a descending curve. By placing a high terminal cost at other singular points, one can prohibit trajectories from terminating at these points. Then the surface solution will only be “learned” from the concave singular points. Furthermore, if the heights of the concave singular points are known, e.g., using stereo, then this can be specified in the algorithm by setting the terminal costs at these points equal to their heights. Since the singular points are distinctive, it is likely that their heights, and the local nature of the surface, can be determined easily from stereo.

The dynamical programming equation corresponding to the cost in eq. 4.20 is exactly the same as eq. 3.16, as is easily seen. The algorithm differs only in the initial condition for  $U^h$ : clearly,  $U^h$  should be set initially to  $g(\phi)$ , not 0 as before. Thus, from the optimal control viewpoint, the choice of initial values for  $U^h$  in the iterative algorithm has a concrete and intuitive interpretation.

## 5. Proof of Equivalence

In this section we will assume the situation of *vertical light*, as described in Section 2. For this case (and under suitable assumptions) the height function has a representation in terms of an associated calculus of variations problem. For the general situation that allows *oblique light* there is a representation in terms of a differential game, as discussed in the next section.

For the case of vertical light the data available for the determination of the function  $z(\cdot)$  is encoded in the intensity function  $I(\mathbf{x}, \mathbf{y})$  determined by eq. 2.1.  $I$  is well defined at all points  $(\mathbf{x}, \mathbf{y})$  where  $z(\cdot)$  is differentiable. We will always assume that the function  $I(\cdot)$  is defined on a bounded open set of the form  $G = \cap_{i=1}^N G_i$ ,  $N < \infty$ , where each  $G_i$  has a  $C^1$  boundary  $\partial G_i$ . Let  $\hat{n}_i(\mathbf{x}, \mathbf{y})$  denote the inward normal to  $G_i$  at  $(\mathbf{x}, \mathbf{y}) \in \partial G_i$ . First consider the following situation.

**Assumption 5.1** 1.  $z(\cdot)$  is  $C^1$  on  $\bar{G}$ .

2. There is exactly one point  $(\tilde{x}, \tilde{y})$  such that  $\nabla z(\tilde{x}, \tilde{y}) = 0$ .

3.  $(\tilde{x}, \tilde{y})$  is a local minimum.

4.  $\nabla z(\mathbf{x}, \mathbf{y}) \cdot \hat{n}_i(\mathbf{x}, \mathbf{y}) < 0$  whenever  $(\mathbf{x}, \mathbf{y}) \in \partial G \cap \partial G_i$ .

(4) implies that the steepest descent direction is always inward on the boundary. We next define a calculus of variations problem. Fix  $(\mathbf{x}, \mathbf{y}) \in \bar{G}$ , and set

$$U(\mathbf{x}, \mathbf{y}) = \inf \int_0^\tau L(\phi(s), \dot{\phi}(s)) ds. \quad (5.21)$$

Here  $\tau = \inf\{t : \phi(t) = (\tilde{x}, \tilde{y})\}$ , and the infimum is over all piecewise continuously differentiable paths  $\phi : [0, \infty) \rightarrow \bar{G}$  that satisfy  $\phi(0) = (\mathbf{x}, \mathbf{y})$ . The variational integrand  $L(\cdot)$  is given by

$$\begin{aligned} L((\mathbf{x}, \mathbf{y}), (u, v)) &= \frac{1}{2} (u^2 + v^2) + \frac{1}{2} \left( \frac{1}{I(\mathbf{x}, \mathbf{y})^2} - 1 \right) \\ &= \frac{1}{2} (u^2 + v^2) + \frac{1}{2} |\nabla z(\mathbf{x}, \mathbf{y})|^2. \end{aligned}$$

We follow the usual convention of defining  $\inf \emptyset = +\infty$ . Thus if  $\phi(t) \neq (\tilde{x}, \tilde{y})$  for all  $t$ , then  $\tau = +\infty$ .

**Theorem 5.2** Under the conditions of Assumption 5.1 we have

$$z(\mathbf{x}, \mathbf{y}) - z(\tilde{x}, \tilde{y}) = U(\mathbf{x}, \mathbf{y}).$$

**Proof.** Let  $\phi(\cdot)$  be any piecewise continuously differentiable path that starts as  $(\mathbf{x}, \mathbf{y})$ . For all  $\varepsilon \geq 0$  define

$$\tau^\varepsilon = \inf\{t : |\phi(t) - (\tilde{x}, \tilde{y})| \leq \varepsilon\}.$$

Fix  $\delta > 0$  and choose  $\varepsilon > 0$  such that

$$z(\mathbf{x}, \mathbf{y}) \leq z(\tilde{x}, \tilde{y}) + \delta$$

for  $|(\mathbf{x}, \mathbf{y}) - (\tilde{x}, \tilde{y})| \leq \varepsilon$ .

To prove  $z(\mathbf{x}, \mathbf{y}) - z(\tilde{x}, \tilde{y}) \leq U(\mathbf{x}, \mathbf{y})$ , we consider two cases. First assume  $\tau^\varepsilon = +\infty$ . By Assumption 5.1 there exists  $c > 0$  such that

$$L((\mathbf{x}, \mathbf{y}), (u, v)) \geq c$$

for all  $(\mathbf{x}, \mathbf{y})$  satisfying  $|(\mathbf{x}, \mathbf{y}) - (\tilde{x}, \tilde{y})| \geq \varepsilon$  and all  $(u, v) \in \mathbf{R}^2$ . Thus, in such a case

$$\int_0^\tau L(\phi(s), \dot{\phi}(s)) ds = \int_0^{\tau^\varepsilon} L(\phi(s), \dot{\phi}(s)) ds = +\infty.$$

Next assume  $\tau^\epsilon < \infty$ . By the chain rule,

$$\frac{d}{dt} [-z(\phi(t))] = -\nabla z(\phi(t)) \cdot \dot{\phi}(t) \leq \frac{1}{2} |\dot{\phi}(t)|^2 + \frac{1}{2} |\nabla z(\phi(t))|^2$$

almost surely in  $t$ . Therefore

$$\begin{aligned} z(\mathbf{x}, \mathbf{y}) - z(\tilde{\mathbf{x}}, \tilde{\mathbf{y}}) &\leq z(\mathbf{x}, \mathbf{y}) - z(\phi(\tau^\epsilon)) + \delta \\ &= -[z(\phi(\tau^\epsilon)) - z(\phi(0))] + \delta \\ &= \int_0^{\tau^\epsilon} -\nabla z(\phi(t)) \cdot \dot{\phi}(t) dt + \delta \\ &\leq \int_0^{\tau^\epsilon} L(\phi(t), \dot{\phi}(t)) dt + \delta \\ &\leq \int_0^\tau L(\phi(t), \dot{\phi}(t)) dt + \delta. \end{aligned}$$

Sending  $\delta \rightarrow 0$  we obtain  $z(\mathbf{x}, \mathbf{y}) - z(\tilde{\mathbf{x}}, \tilde{\mathbf{y}}) \leq U(\mathbf{x}, \mathbf{y})$ .

To prove  $z(\mathbf{x}, \mathbf{y}) - z(\tilde{\mathbf{x}}, \tilde{\mathbf{y}}) \geq U(\mathbf{x}, \mathbf{y})$ , let  $\phi(\cdot)$  be a solution (note that there may not be uniqueness since  $z$  is only assumed  $C^1$ ) to the equation

$$\dot{\phi}(t) = -\nabla z(\phi(t)), \quad \phi(0) = (\mathbf{x}, \mathbf{y}).$$

By Assumption 5.1  $\phi(\cdot)$  never touches  $\partial G$  for  $t > 0$ , and therefore the solution is well defined for all  $t > 0$ . Let  $\tau = \inf\{t : \phi(t) = (\tilde{\mathbf{x}}, \tilde{\mathbf{y}})\}$  and let  $a \wedge b$  denote the smaller of  $a$  and  $b$ . For any  $t < \infty$ , we have

$$\begin{aligned} z(\mathbf{x}, \mathbf{y}) - z(\tilde{\mathbf{x}}, \tilde{\mathbf{y}}) &\geq z(\phi(0)) - z(\phi(t \wedge \tau)) \\ &= -[z(\phi(t \wedge \tau)) - z(\phi(0))] \\ &= \int_0^{t \wedge \tau} -\nabla z(\phi(s)) \cdot \dot{\phi}(s) ds \\ &= \int_0^{t \wedge \tau} |\nabla z(\phi(s))|^2 ds \\ &= \int_0^{t \wedge \tau} L(\phi(s), \dot{\phi}(s)) ds. \end{aligned}$$

Sending  $t \rightarrow \infty$  we conclude that

$$z(\mathbf{x}, \mathbf{y}) - z(\tilde{\mathbf{x}}, \tilde{\mathbf{y}}) \geq \int_0^\tau L(\phi(s), \dot{\phi}(s)) ds \geq U(\mathbf{x}, \mathbf{y}).$$

■

The solution to the calculus of variations problem uniquely identifies the height function up to an overall translation in  $z$ . This ambiguity can be removed by specifying  $z(\tilde{\mathbf{x}}, \tilde{\mathbf{y}})$ .

We next consider a more general situation involving more than one stationary point. Let  $M$  be the set of local minima of  $z(\cdot)$ .

**Assumption 5.3** 1.  $z(\cdot)$  is  $C^1$  on  $\bar{G}$ .

2. The value of  $z(\cdot)$  is known on  $M$ .

3.  $\nabla z(\mathbf{x}, \mathbf{y}) \cdot \hat{n}_i(\mathbf{x}, \mathbf{y}) < 0$  whenever  $(\mathbf{x}, \mathbf{y}) \in \partial G \cap \partial G_i$ .

Define the terminal cost function

$$g(\mathbf{x}, \mathbf{y}) = \begin{cases} z(\mathbf{x}, \mathbf{y}) & \text{if } (\mathbf{x}, \mathbf{y}) \in M, \\ +\infty & \text{otherwise.} \end{cases}$$

Consider the calculus of variations problem

$$U(\mathbf{x}, \mathbf{y}) = \inf \left[ \int_0^\tau L(\phi(s), \dot{\phi}(s)) ds + g(\phi(\tau)) \right]. \quad (5.22)$$

Here the infimum is over all  $\tau < \infty$  and absolutely continuous paths  $\phi : [0, \tau] \rightarrow \bar{G}$  that satisfy  $\phi(0) = (\mathbf{x}, \mathbf{y})$ . Unlike the case of a single stationary point, it is necessary that a terminal cost be included in order to guarantee that trajectories do not get “stuck” at stationary points that are not local minima.

We have the following result for this case.

**Theorem 5.4** *Under the conditions of Assumption 5.3 we have*

$$z(\mathbf{x}, \mathbf{y}) = U(\mathbf{x}, \mathbf{y}).$$

**Remarks on the proof.** The proof is very similar to that of Theorem 5.2 and will only be sketched. Consider any path  $\phi(\cdot)$  which starts at  $(\mathbf{x}, \mathbf{y})$  and for which the cost

$$\int_0^\tau L(\phi(s), \dot{\phi}(s)) ds + g(\phi(\tau)) \quad (5.23)$$

is finite. Boundedness of the cost implies  $\phi(\tau) \in M$ . Suppose  $\phi(\tau) = (\hat{\mathbf{x}}, \hat{\mathbf{y}})$ . The proof of Theorem 5.2 then shows that  $z(\mathbf{x}, \mathbf{y}) - z(\hat{\mathbf{x}}, \hat{\mathbf{y}}) \leq \int_0^\tau L(\phi(s), \dot{\phi}(s)) ds$ . Together with the definition of  $g(\cdot)$  this implies  $z(\mathbf{x}, \mathbf{y}) \leq U(\mathbf{x}, \mathbf{y})$ .

Next consider the reverse inequality. As in the proof of Theorem 5.2, we would like to construct a particular path  $\phi(\cdot)$  that starts at  $(\mathbf{x}, \mathbf{y})$  so that the cost (5.23) is arbitrarily close to  $z(\mathbf{x}, \mathbf{y})$ . We first note that by a perturbation argument [11,10,13] we can assume that there are at most finitely many points such that  $\nabla z(\mathbf{x}, \mathbf{y}) = 0$ . It can be shown that there exists a dense subset  $D$  of  $\bar{G}$  with the property that whenever the path  $\phi(\cdot)$  satisfies

$$\dot{\phi}(t) = -\nabla z(\phi(t)), \phi(0) \in D,$$

then  $\phi(t)$  converges to a local minimum  $(\tilde{\mathbf{x}}, \tilde{\mathbf{y}})$  of  $z(\cdot)$  as  $t \rightarrow \infty$ . Using the argument of Theorem 5.2 and the fact that  $z(\phi(t))$  is nondecreasing we conclude  $z(\mathbf{x}, \mathbf{y}) \geq U(\mathbf{x}, \mathbf{y})$  for  $(\mathbf{x}, \mathbf{y}) \in D$ . By continuity of both  $z(\cdot)$  and  $U(\cdot)$  (which is easy to prove) we have  $z(\mathbf{x}, \mathbf{y}) \geq U(\mathbf{x}, \mathbf{y})$  for  $(\mathbf{x}, \mathbf{y}) \in \bar{G}$ . ■

Previous uniqueness proofs [1,15,12] assumed that  $z(\mathbf{x}, \mathbf{y})$  was at least  $C^2$ ; here  $z$  is only assumed  $C^1$ . A fortiori, no conditions are placed on the second derivatives of the intensity; in particular, the singular points are not required to be “good” or “nondegenerate” [15,12].

## 6. Illumination from a General Direction

For a Lambertian surface, the image irradiance equation for the intensity is:

$$I(\mathbf{x}, \mathbf{y}) = \hat{L} \cdot \frac{(-z_x, -z_y, 1)}{(1 + z_x^2 + z_y^2)^{1/2}}, \quad (6.24)$$

where  $\hat{L}$  is a unit vector giving the light source direction, and  $z_x, z_y$  are partial derivatives of the height. For simplicity and w.l.o.g., we take the  $x$ -component of  $\hat{L}$  to be zero. After some algebra, this equation may be rewritten as:

$$I^2 z_x^2 + J z_y^2 + 2L_z L_y z_y + (I^2 - L_z^2) = 0, \quad (6.25)$$

with  $J(\mathbf{x}, \mathbf{y}) \equiv I^2(\mathbf{x}, \mathbf{y}) - L_z^2$ .

We define a new variable  $\xi \equiv (\mathbf{x}, y, z) \cdot \hat{L}$ ;  $\xi$  measures the "height" along the light direction rather than the viewer direction  $\hat{z}$ . This is done so that the local cost at singular points will be zero, like  $V$  previously, causing optimal trajectories to terminate at these points. We have:

$$\xi_x = L_z z_x, \quad \xi_y = L_y + L_z z_y. \quad (6.26)$$

Substituting in the previous equation yields

$$I^2 \xi_x^2 + J \xi_y^2 + 2(1 - I^2) L_y \xi_y - (1 - I^2) = 0. \quad (6.27)$$

$J$ , the coefficient of  $\xi_y^2$ , is positive in an image region  $B$  that includes the singular points. When  $I^2 = L_y^2$ , the angle between the surface normal and  $\hat{L}$  is large enough so that a normal in the  $\mathbf{x}$ - $y$  plane becomes a possibility—this intensity value can correspond to a point on the occluding boundary.

In the image region  $B$ , we consider a control problem analogous to that of Section 2: a 'particle' initially located at  $(\mathbf{x}, y)$  is controlled using the parameters  $u, v$ :

$$\dot{\mathbf{x}} = I^2(\mathbf{x}, y)u, \quad \dot{y} = J(\mathbf{x}, y)v - (1 - I^2(\mathbf{x}, y))L_y. \quad (6.28)$$

$u, v$  are chosen to infimize a cost function for the particle's trajectory

$$U(\mathbf{x}, y, T) = \inf_{(u,v)} \frac{1}{2} \int_0^T ds \left( I^2(\mathbf{x}, y)u^2 + J(\mathbf{x}, y)v^2 + (1 - I^2(\mathbf{x}, y)) \right). \quad (6.29)$$

As before the integrand is nonnegative throughout the region  $B$ , and the local cost  $1 - I^2$  vanishes at singular points. In the vertical-light case  $L_y = 0$ , the cost of eq. 2.4 can be recovered by dividing the above equation by  $I^2$ .

This control problem is essentially equivalent to the one previously considered, and results similar to those of the previous sections are easily obtainable. In particular, by a Schwarz inequality argument similar to that of the last section,

$$\begin{aligned} \frac{d}{dt} [-\xi(\phi(t))] &= -\nabla \xi(\phi(t)) \cdot \dot{\phi}(t) = -\xi_x I^2 u - \xi_y (Jv - (1 - I^2)L_y) \\ &\leq \frac{1}{2} \left( I^2 u^2 + Jv^2 + I^2 \xi_x^2 + J \xi_y^2 + 2\xi_y(1 - I^2)L_y \right) \\ &= \frac{1}{2} \left( I^2 u^2 + Jv^2 + 1 - I^2 \right), \end{aligned} \quad (6.30)$$

which is just the integrand of eq. 6.29. This gives the necessary generalization for the rigorous proof of equivalence. Similarly, an algorithm can be defined in the same way as before, and will recover the correct solution near concave (or convex) singular points.

In the image region where  $I^2 - L_y^2 < 0$ , the optimal control representation of the problem no longer suffices. Instead, we must use a representation in terms of a *differential game* (see e.g. [2]). However, it is a particularly simple differential game, in which the opposing controllers effectively direct the 'particle' motion in orthogonal directions, and where the cost also splits into a sum of terms depending on the different control parameters. Thus, the Isaacs condition and the existence of a "value" follow.

The 'particle' dynamics for the differential game is:

$$\dot{\mathbf{x}} = I^2 u, \quad \dot{y} = J(\theta(J)v_1 + \theta(-J)v_2) - (1 - I^2)L_y, \quad (6.31)$$

where

$$\theta(x) = \begin{cases} 1 & \text{if } x \geq 0, \\ 0 & \text{if } x < 0. \end{cases} \quad (6.32)$$

The player associated with  $u$  and  $v_1$  seeks to minimize the value function of the game, while the  $v_2$  player seeks to maximize it. The value that opposing players attempt to control is

$$U(\phi, t) \equiv \frac{1}{2} \int_0^T ds \left( I^2 u^2 + J(\theta(J)v_1^2 + \theta(-J)v_2^2) + (1 - I^2) \right). \quad (6.33)$$

A precise description of the differential game is somewhat technical (see e.g. [2]). Here we will simply note that the properly defined value gives the height function (under suitable conditions), and that an algorithm on a discrete grid for approximating this value function can be derived that is similar to the algorithm for vertical light.

## 7. Experiments

Fig. 1 displays a 32 by 32 surface which is assumed to be imaged from above. The image intensity is computed using the discretization of the derivative implicit in eqs. 3.16, 3.17. The image has one singular point. Assuming vertical light, the algorithm converges to the correct solution to within, on average, one part in  $10^6$  after 70 iterations. This could be improved using Gauss-Seidel, as noted earlier. In general, we expect the convergence time to be on the order of the maximum length of an optimal trajectory. When  $\Delta t$  in eq. 3.16 is adjusted to its maximal value consistent with stable convergence (this can be determined from eq. 3.16 itself), then an optimal trajectory jumps approximately one lattice site per iteration. When the number of iterations becomes greater than the maximum trajectory length, then all image points are able to “learn” their heights from the singular points. For the given surface, the maximal trajectory length is on the order of 32, since trajectories starting at the image corners must zigzag to the singular point at the center of the image. This surface was also successfully reconstructed assuming oblique light at an angle  $37^\circ$  to the vertical.

The algorithm has also been applied to a noisy image of this surface; the result is a noisy approximation of the surface. The convergence time is longer since the steepest descent curves lengthen due to wiggling.

For comparison, Figs. 2, 3 display the result of applying our implementation of Horn’s algorithm [4] to a similar surface. The intensity is computed differently than before, using the discrete derivatives appropriate for this algorithm. Even after 3072 iterations, the algorithm has not converged to the correct solution. We have also implemented the variational algorithms of [8] and [16], and applied them to this surface with similar results. As also noted by [9], standard variational algorithms often give a wrong, saddle-shaped surface, when presented with a simple image containing one singular point.

Fig. 4 shows a more complicated 128 by 128 surface. The intensity was computed as for Fig. 1. The algorithm this time incorporated a terminal cost—an initial value for  $U$ —which was large everywhere but at the concave singular points. At these points,  $U$  was initialized to the known height values. For vertical light, the algorithm converged to a perfect reconstruction of the original surface within 150 iterations. As expected, the convergence time is on the order of the longest optimal trajectory. This surface was also reconstructed assuming oblique light at an angle of  $17.5^\circ$  to the vertical.

Fig. 5 shows the result for vertical light of applying the algorithm without the terminal cost. The algorithm reconstructs a surface that is locally concave at all singular points; it is correct in the neighborhood of those singular points where the surface is in fact locally concave. Note the sharp orientation discontinuities at the boundaries between the regions associated with different singular points.

Finally, Fig. 6 shows the result of applying the algorithm to an “impossible image” similar to the one in [4], Fig. 10.

## 8. Acknowledgments

This work was supported by the Defense Advanced Research Projects Agency under grants F30602-87-C-0140 and DACA76-89-C-0017, and by the National Science Foundation under grants DCR-8500332 and IRI-9014698 and NSF-DMS-8902333.

## References

1. A. R. Bruss, "The Eikonal Equation: Some Results Applicable to Computer Vision," *Journal of Math. Phys.* 23(5): 890-896, May 1982.
2. R. J. Elliott, *Viscosity Solutions and Optimal Control*, Longman Scientific and Technical, New York, NY: 1987.
3. B.K.P. Horn, "Obtaining Shape from Shading Information," in *The Psychology of Computer Vision*, P. H. Winston (ed.), McGraw Hill: New York, 1975, pp. 115-155.
4. B.K.P. Horn, "Height and Gradient From Shading," *International Journal of Computer Vision* Vol. 5 No. 1, pp. 37-75, 1990.
5. B. K. P. Horn and M. J. Brooks, "The Variational Approach to Shape from Shading," *Computer Vision, Graphics, and Image Processing*, Vol. 33, pp. 174-208, 1986.
6. K. Ikeuchi and B. K. P. Horn, "Numerical Shape from Shading and Occluding Boundaries," *Artificial Intelligence*, Vol. 17, Nos. 1-3, pp. 141-184, August 1981.
7. H. J. Kushner, "Numerical methods for stochastic control problems in continuous time," *SIAM J. Control and Optimization*, Vol. 28, 1990.
8. Y. G. Leclerc and A. F. Bobick, "The Direct Computation of Height from Shading," *Proc. IEEE Conference on Computer Vision and Pattern Recognition*, Lahaina, Maui, Hawaii, 1991, pp. 552-558.
9. Y. G. Leclerc and A. F. Bobick, *personal communication*.
10. J. Milnor, *Morse Theory*, Annals of Mathematics Studies 51. Princeton University: New Jersey, 1970.
11. J. Oliensis, "Shape from Shading as a Partially Well-Constrained Problem," *Computer Vision, Graphics, and Image Processing: Image Understanding*, to appear.
12. J. Oliensis, "Uniqueness in Shape From Shading," *The International Journal of Computer Vision*, to appear.
13. J. Palis and W. de Melo, *Geometric Theory of Dynamical Systems*. Springer-Verlag: NY, 1982.
14. B. V. H. Saxberg, "An Application of Dynamical Systems Theory to Shape From Shading," in *Proc. DARPA Image Understanding Workshop*, Palo Alto, CA, May 1989, pp. 1089-1104.
15. B. V. H. Saxberg, "A Modern Differential Geometric Approach to Shape from Shading," MIT Artificial Intelligence Laboratory, TR 1117, 1989.
16. R. Szeliski, "Fast Shape from Shading," *Computer Vision, Graphics, and Image Processing: Image Understanding*, Vol. 53, pp. 129-153, 1991.

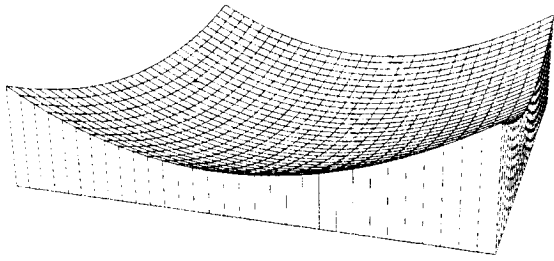


Fig. 1. Parabolic surface.

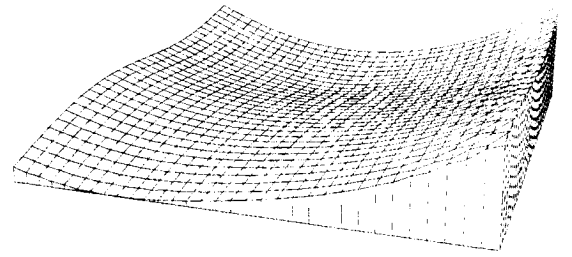


Fig. 2. 128 iterations of Horn's algorithm.

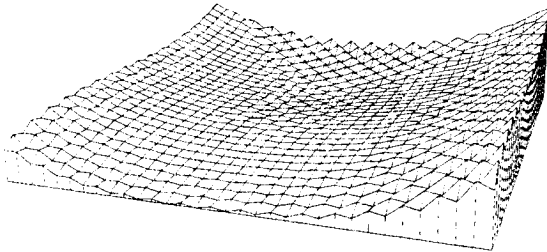


Fig. 3. 3072 iterations of Horn's algorithm.

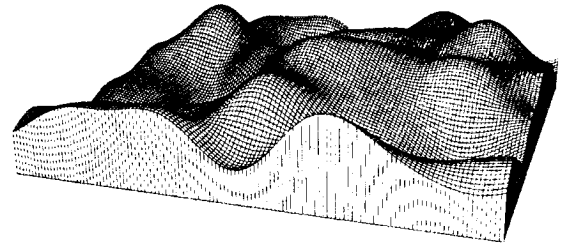


Fig. 4. Complex surface.

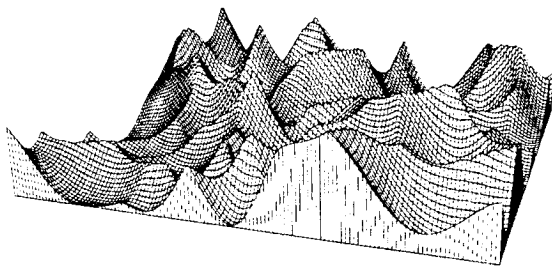


Fig. 5. Result with no terminal cost.

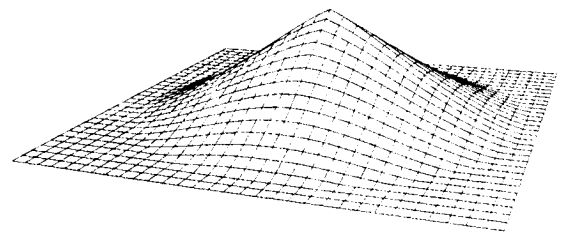


Fig. 6. Reconstruction for an "impossible" image.